Journal of GeoEngineering, Vol. 9, No. 2, pp. 45-53, August 2014
http://dx.doi.org/10.6310/jog.2014.9(2).1

WEDGE SIZE ISSUES ON CALCULATING SEISMICALLY INDUCED LATERAL EARTH PRESSURE FOR RETAINING STRUCTURES – AN OVERVIEW AND A NEW SIMPLE APPROACH

Chi-Chin Tsai [1] and Erik J. Newman [2]

ABSTRACT

Case history data and data from recent experiments indicate that currently used methods for evaluating seismically induced lateral earth pressure are conservative and can potentially lead to overdesign. This paper reviews commonly used methods (*e.g.*, Mononobe-Okabe, M-O, method) and discusses wedge size issues in the calculation of seismically induced lateral earth pressures for retaining structures. Unlike the M-O method, wherein the critical wedge is dependent on seismic intensity, a fixed-wedge approach is proposed in this study on the basis of observations from case histories, experiments, and FEM analysis results. The earth pressures calculated by the proposed procedure agree well with recent experiments. Hence, the fixed-wedge approach is recommended in lieu of the M-O method.

Key words: Seismic, earth pressure, retaining structure, wedge size, Mononobe-Okabe method.

1. INTRODUCTION

The seismic response of retaining structures is a complex soil structure interaction problem. Wall movements and dynamic earth pressures depend on numerous details, including the responses of the soil underlying the wall and backfill, the inertial and flexural responses of the wall itself, and the nature of the input motions (Al Atik and Sitar 2010). The currently used approach for evaluating the seismic performance of retaining structures has been established in the pioneering studies of Okabe (1926) and Mononobe and Matsuo (1929). The Mononobe-Okabe (M-O) method is based on Coulomb's theory of static soil pressure, and was originally developed for gravity walls that retain cohesionless backfill materials. The M-O method and its adaptation by Seed and Whitman (S-W method 1970) are widely practiced and employed as standards. The latest NCHRP report on the subject (Anderson *et al*. 2009) also recommends the use of the M-O method in designing conventional retaining walls.

Nevertheless, studies have raised questions on the general applicability of this methodology. Several analytical studies and experiments, including that of Koseki *et al.* (1998a), Nakamura (2006), Psarropoulos *et al.* (2005), Al Atik and Sitar (2010), and Watanabe *et al.* (2011), suggest that the M-O method leads to conservative estimates of dynamic earth pressures. By contrast, for retaining walls with low importance, the seismic design is usually omitted by assuming that a wall designed for static conditions with an acceptable factor of safety will have sufficient capacity to resist seismic loads (*e.g.*, JRA 1987; Caltrans 2010). Case histories have proven that cantilever retaining structures designed for no or inadequate seismic loading have performed reasonably well during past earthquakes (Clough and Fragaszy 1977; Gazetas *et al.* 2004; Koseki *et al.* 1998b; Lew *et al.* 1995).

Given the increased awareness of seismic risks and an improved understanding of the magnitude of potential ground motions, retaining structures in regions near seismic sources are required to be designed with consideration to high ground motion intensities. Several failure cases of retaining walls during the 1995 Hyogoken-Nanbu Earthquake and the 1999 Chi-Chi Earthquake indicated that the peak ground accelerations (PGA) experienced by the structures were high (up to 0.8 g) (Tatsuoka *et al.* 1996). Applying the M-O method under such large seismic loads may lead to large earth forces with a typical friction angle of backfill ranging from 30° to 40°, thus making the structural design expensive. Furthermore, the M-O method becomes inoperative when the seismic load exceeds a certain limit.

This study primarily reviews commonly used methods (*i.e.*, M-O method) and discusses their limitations in calculating dynamic earth pressures because of conditions wherein unreasonable wedge sizes are estimated. On the basis of the observed failure planes from recent case histories, experiments by other researchers, and numerical simulations in this study, we propose a simple fixed-wedge procedure to accurately calculate dynamic earth pressures under small to large seismic loads. Earth pressures calculated by using the proposed procedure agree well with the measurements obtained by experiments with seismic loads of up to 1.0 g. This result validates the applicability of the proposed method in engineering design.

2. M-O METHOD AND ITS APPLICATION

2.1 Review of the M-O Method

The M-O method is based on the studies of Okabe (1926) and Mononobe and Matsuo (1929) following the 1923 Kanto Earthquake in Japan. This method is originally intended for gravity walls that retain cohesionless backfill materials and is the most commonly used approach in determining seismically induced earthquake pressure on a retaining structure.

Manuscript received February 28, 2014; revised June 27, 2014; accepted June 30, 2014.
[1] Assistant Professor (corresponding author), Department of Civil Engineering, National Chung Hsing University, 250 Kuo Kuang Rd., Taichung 402, Taiwan (e-mail: tsaicc@nchu.edu.tw).
[2] Project Engineer, URS Corporation, Suite 800, 1333 Broadway, Oakland, CA 94612, USA.

The M-O method uses pseudo-static analysis based on Coulomb wedge theory to calculate active and passive earth pressures. This method includes additional vertical and horizontal seismic forces (Fig. 1). By using force equilibrium, the total active thrust P_{AE} per unit length of the wall is determined as follows:

$$P_{AE} = 0.5\gamma H^2 (1-k_v) K_{AE} \tag{1}$$

where

$$K_{AE} = \frac{\cos^2(\varphi-\psi-\alpha)}{\cos\psi\cos^2\alpha\cos(\delta+\alpha+\psi)\left[1+\sqrt{\frac{\sin(\varphi+\delta)\sin(\varphi-\psi-\beta)}{\cos(\delta+\alpha+\psi)\cos(\beta-\alpha)}}\right]^2} \tag{2}$$

γ = unit weight of the soil; H = height of the wall; φ = internal friction angle of the soil; δ = friction angle between the wall and the soil; α = slope of the wall relative to vertical; $\psi = \tan^{-1}(k_h / (1 - k_v))$, where k_v and k_h are the respective coefficients of vertical and horizontal seismic accelerations in a fraction of gravitational acceleration. The angle θ defining the orientation of the failure plane can be calculated as follows (Koseki *et al.* 1998b):

$$\cot(\theta-\beta) = -\tan(\varphi+\delta+\alpha-\beta) + \sec(\varphi+\delta+\alpha-\beta)\sqrt{\frac{\cos(\alpha+\delta+\psi)\sin(\varphi+\delta)}{\cos(\alpha-\beta)\sin(\varphi-\beta-\psi)}} \tag{3}$$

Equation (1) represents the total active thrust on the wall during seismic loading. The point of application of the resulting force is typically assumed to be at 2/3 H below the top of the wall. Seed and Whitman (1970) simplified the calculation by separating the total force on the wall into static and dynamic components. Their proposed simplified expression for the dynamic increment (component) of the active thrust is expressed as follows:

$$\Delta P_{AE} = 1/2\,\gamma H^2 \Delta K_{AE} \quad \text{and} \quad \Delta K_{AE} \approx 3/4\,k_h \tag{4}$$

where ΔK_{AE} is the change in the earth pressure coefficient caused by seismicity. This approximation is asymptotically tangential to the M-O solution at an acceleration below 0.4 g under the conditions of the vertical wall, level backfill, and $\varphi = 35^o$. The approximation of ΔK_{AE} as 3/4 k_h implies that the seismic earth pressure increment is caused by the inertia force of a "fixed" wedge with a height of H and a base width of 3/4 H regardless of the magnitude of seismic load.

2.2 Limitation of the M-O Method

The angle of the potential sliding surface (θ) in the M-O method (Fig. 1) varies with the magnitude of the input seismic coefficient. The dynamic earth pressure obtained by the M-O method becomes unavailable when the value inside the square root term of Eq. (2) becomes negative, that is

$$\varphi - \psi - \beta < 0 \tag{5}$$

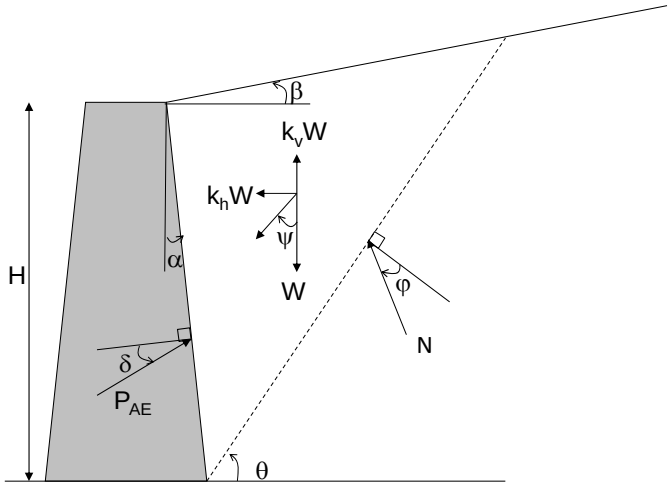

Fig. 1 M-O method

Equation (5) implies that it occurs when the horizontal seismic coefficient k_h exceeds a certain limit:

$$k_h > (1-k_v)\tan(\varphi-\beta) \tag{6}$$

This occurrence is caused by the flattening of the potential sliding plane with increasing horizontal seismic coefficient. When k_h exceeds the limit, the potential sliding plane becomes too flat to intersect with the surface of the backfill. Thus, the size of the critical wedge becomes infinite, and no solution can be obtained. Such a condition is likely to occur when the backfill is sloped ($\beta > 0$) or loose (φ is small) (Eq. (5)). By taking a 6.5 m high vertical wall with a level backfill as an example, the potential failure planes corresponding to different k_h values are shown in Fig. 2(a). The wedge sizes are reasonable when k_h is less than 0.3 g but become unreasonable when k_h is greater than 0.5 g. The potential sliding plane eventually becomes parallel to the ground surface, and no wedge can be found.

A dramatic change in wedge size can lead to a significant increment in dynamic earth pressure. Figure 2(b) presents the seismic earth pressure increments in terms of ΔK_{AE} for various k_h. ΔK_{AE} is back-calculated through Eq. (4) given the seismic earth pressure increment ΔP_{AE}, which is the difference between the seismic earth pressure based on Eqs. (1) and (2) and the static earth pressure. The dynamic increment of the active thrust increases linearly and rapidly with a k_h of less than and more than 0.3 g, respectively. Therefore, this limitation in determining the potential failure plane is one possible reason behind the conservative estimations of seismic earth pressures that the M-O method provides. This limitation occurs because the M-O method calculates seismic earth pressures by the force equilibrium of the rigid wedge without considering the flexibility of backfill materials (*i.e.*, stress-strain compatibility) and construction/loading sequences. The potential failure plane will not develop infinitely if the effect of strain localization on the backfill soil and loading histories is considered (Koseki *et al.* 1998b).

Similar limitations can be found in the limit-equilibrium analysis of the stability of an embankment atop a soft foundation under a pseudo-static condition. The critical failure plane tends to increase with increasing k_h. The potential failure plane can become unreasonably large given a large k_h if only the force

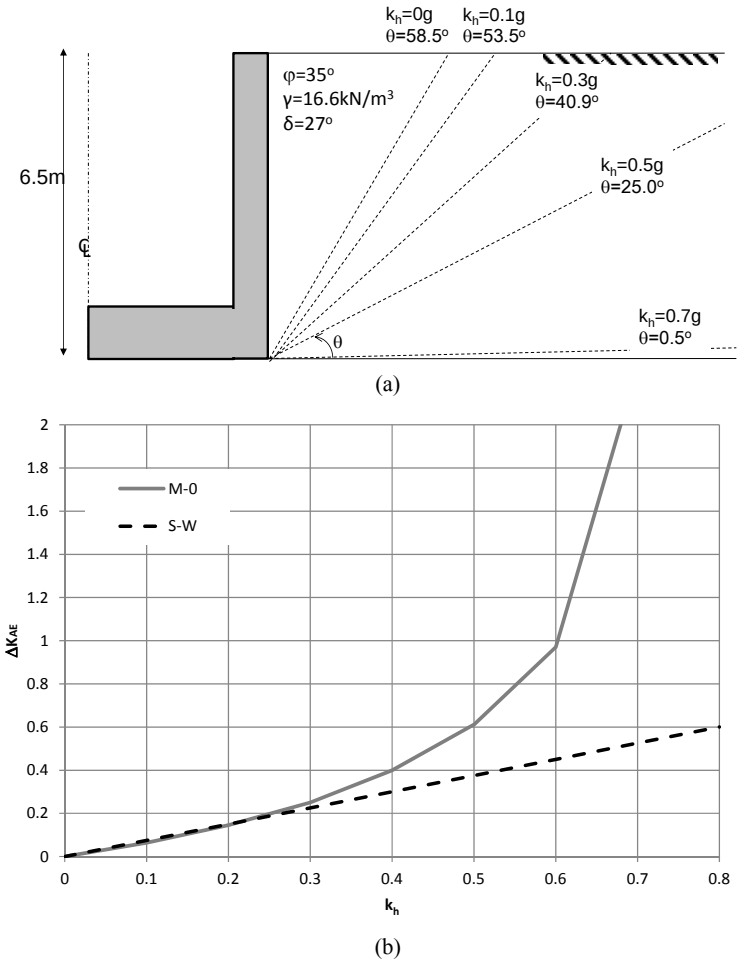

Fig. 2 (a) Potential failure planes and (b) seismic earth pressure increment coefficient corresponding to different horizontal seismic coefficients

equilibrium of a potential rigid failure block is considered without the flexibility of the foundation material. By contrast, the potential failure plane will only develop near the toe of the embankments if the strain localization is considered. Therefore, a fixed failure circle based on the static result is often used to determine yield acceleration in engineering practice to overcome this limitation.

In addition to the main drawback described above, the M-O method can overestimate the dynamic earth pressure on the retaining wall because of the following factors:

1. Scattering factor: The equivalent seismic loading on the critical wedge is different from and usually less than the base motions because of the flexibility of the wedge. The low seismic loading on the critical wedge is more pronounced under higher walls and stronger motions (Anderson *et al.* 2009).
2. Time-dependent factor: The PGA (maximum force) occurs shortly and only once. The PGA also has an insufficient duration to cause significant wall movements. A pseudo-static analysis that assume the seismic coefficient equals the PGA provides the upper-bound results.
3. Yielding of wall: The wall allows some degree of movement, thus reducing seismic loading. The yielding of the wall implies that the wall can tolerate certain displacements under seismic conditions.

Without considering these factors, the M-O method with free-field PGA as the input seismic coefficient can yield a conservative estimate of dynamic earth pressures. To rationally approximate actual seismic earth pressures, the current AASHTO LRFD Bridge Design Specifications (AASHTO 2013) suggests that the seismic coefficient should be equal to half of the PGA in the design of non-gravity cantilever walls. However, the selection of a proper seismic coefficient for pseudo-static analysis of the wall-soil system is beyond the scope of this study. We will focus on the effect of strain localization (*i.e.*, wedge size) to overcome the limitation described earlier in the pseudo static and limit-equilibrium approaches.

3. WEDGE SIZE OBSERVED FROM CASE HISTORIES, LABORATORY TESTS, AND FEM SIMULATION

Only a small amount of outward wall displacement is needed to trigger the active failure of the backfill. For a wall rotating about its base, the outward displacement at the top of the wall is about 0.1% to 0.4% of the wall height from an at-rest condition (Terzaghi 1920; Fang 1991). Therefore, the active wedge in the backfill is likely to develop at a static condition or at a low seismic load. Shear resistance can remain mobilized along a previously formed failure plane for subsequent seismic loads. The hypothesis implies that the failure wedges should be similar regardless of the magnitude of the seismic loading; this hypothesis contradicts the result of the M-O method. To support this hypothesis, the behavior of the retaining wall (*i.e.*, the angle of failure plane θ) subjected to seismic loading is explored by using case histories, laboratory tests, and FEM simulation.

3.1 Case Histories during the 1999 Chi-Chi Earthquake and the 1995 Hyogoken-Nanbu Earthquake

Fang *et al.* (2003) documented the failures of quay walls, masonry walls, gravity walls, modular-block retaining walls, and reinforced earth retaining structures during the 1999 Chi-Chi Earthquake. These field observations suggest that the failure plane occurs locally instead of developing infinitely. Tatsuoka *et al.* (1996 and 1998) summarized the performance of conventional and reinforced soil retaining walls during the 1995 Hyogoken-Nanbu earthquake. One key finding is that the orientation of the failure plane is steeper than the theoretical value of the M-O method for the given PGA at the base. Figure 3(a) shows one failure case of a leaning-type wall at the Sumiyoshi site. The failure plane in the backfill of a damaged railway retaining wall is at an angle of 80° to the horizontal. Given a wall inclination angle of 32° and a friction angle of 35°, the theoretical angle of the failure plane at the static condition is 78.5°, which is analogous to the observation. The second case is a gravity-type wall at the Ishiyagawa site (Fig. 3(b)). Given the conditions of the wall inclination angle $\alpha = -17^{\circ}$ and friction angle $\varphi = 35^{\circ}$, the calculated angle of the failure plane at the static condition is 54°, which is consistent with the field observation during the earthquake. Both sites likely experienced strong ground shaking of up to 0.45 g (*i.e.*, k_h = 0.45 g). However, the observed critical failure planes are similar to the theoretical failure planes under the static condition and not the failure planes determined by the M-O method.

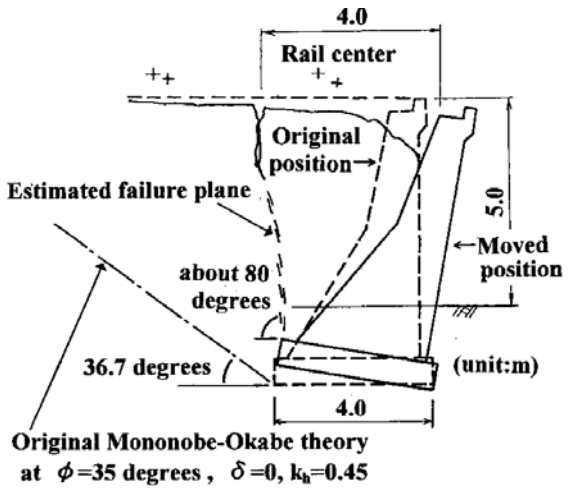

(a)

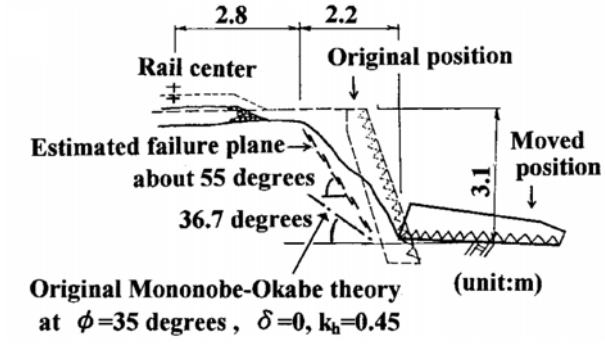

(b)

Fig. 3 Failure cases at the (a) Sumiyoshi site and (b) Ishiyagawa site during the 1995 Hyogoken-Nanbu Earthquake (Tatsuoka *et al.* 1998)

3.2 Finite Element Method Simulation

A stress-strain deformation analysis by using FEM is performed to investigate the development of a potential failure wedge behind the retaining wall under different seismic conditions. The FE approach can accurately model in-situ stresses, which is not considered in the M-O method, prior to seismic loading. In this study, a 6.5 m-high U-shaped wall similar to that in the centrifuge test (Al Atik and Sitar 2010) is modeled by the FEM program PLAXIS. The same model parameters obtained in the centrifuge test (listed in Table 1) are also used. FEM analysis is performed under pseudo-static conditions to mimic the M-O approach, wherein horizontal body forces proportional to gravity are applied in addition to the vertical gravity loads. However, seismic coefficient k_h is applied only after the wall–backfill system reaches equilibrium under gravity load instead of at the start of analysis with gravity load. This staged analysis allows the wall to deform under static conditions such that strains in the backfill can develop prior to the seismic event. Such conditions are typically encountered in reality. Kontoe *et al.* (2013) explored the sensitivity of pseudo-static analysis results on the adopted mesh size in FEM analysis. A generalized layer failure mechanism caused by shearing of pseudo-static force can be developed simultaneously with the wall mechanism for problems with high seismic coefficient values. Thus, the mesh size is adjusted accordingly to avoid the interference of a generalized layer failure for large seismic loads.

Table 1 Parameters used in FEM analysis

Model parameter	Parameter value
Mass density (kg/m^3)	1692
Shear modulus (kPa)	5.30×10^4
Poisson's ratio	0.3
Friction angle (deg)	35
Interphase friction angle (deg)	27

The shear strain increments in each staged analysis are presented in Fig. 4. The reason to use shear strain increment $\Delta\gamma_{xy}$ (caused by wall lateral movement and k_h) is to separate them from the initial shear strain due to k_o condition. Such presentation is commonly used to illustrate shear-induced failure mechanism in numerical modeling. Figure 4(a) shows the shear strain increments resulting from wall movements during construction under gravity load (static condition). The presence of high shear strain increments indicates the location of the potential failure plane; this observation agrees well with the theoretical critical plane (red dotted line) based on the Coulomb method. Figures 4(b) and 4(c) show additional shear strains under pseudo-static conditions by using k_h = 0.3 and 0.5 g, respectively. The size of the potential failure wedge under k_h = 0.3 g is slightly larger than that under the static condition and is between those predicted by the Coulomb and M-O methods. The size of the potential failure wedge increases to some extent with increasing seismic intensity (k_h = 0.5 g). However, the change is not as significant as the change predicted by the M-O method. The FEM results indicate that the size of the wedge appears to change insignificantly when a staged stress–strain deformation analysis is performed, in contrast to the predictions of the M-O method.

3.3 Shaking Table Test and Tilt Test

Many researchers have conducted experiments to investigate the complex response of the retaining wall system. A series of model tests have been performed to explore the behavior of the retaining wall under dynamic loading, particularly for strong motions since 1998 (Koseki, *et al*. 1998a; Watanabe *et al*. 2011; Watanabe *et al.* 2003). The small-scale model tests contain shaking table and tilt test models on different types of retaining walls, including gravity-type, leaning-type, cantilever-type, and geosynthetic-reinforced soil retaining wall. The response accelerations of both the wall and backfill layers are recorded, as well as wall displacement, earth pressures in the soil layers, and failure plane in the backfill. The observed orientations of the failure plane in the backfill are summarized in Table 2. The P_{AE} value listed in Table 2 is the overall maximum value in the whole time history of P_{AE} and differs from the value reported by Watanabe *et al.* (2003), who reported the P_{AE} at the moment when maximum equivalent acceleration occurs within the soil wedge.

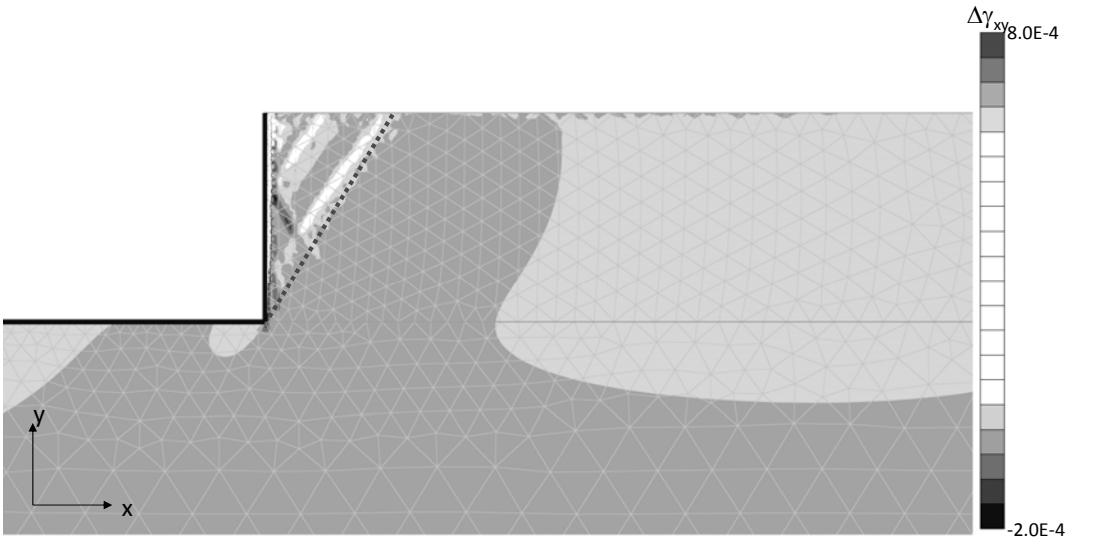

(a)

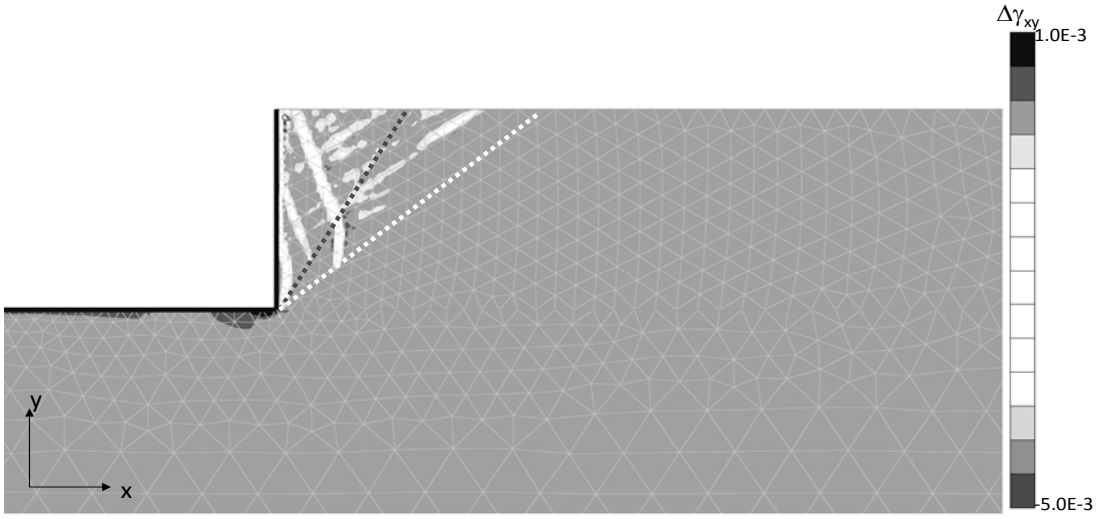

(b)

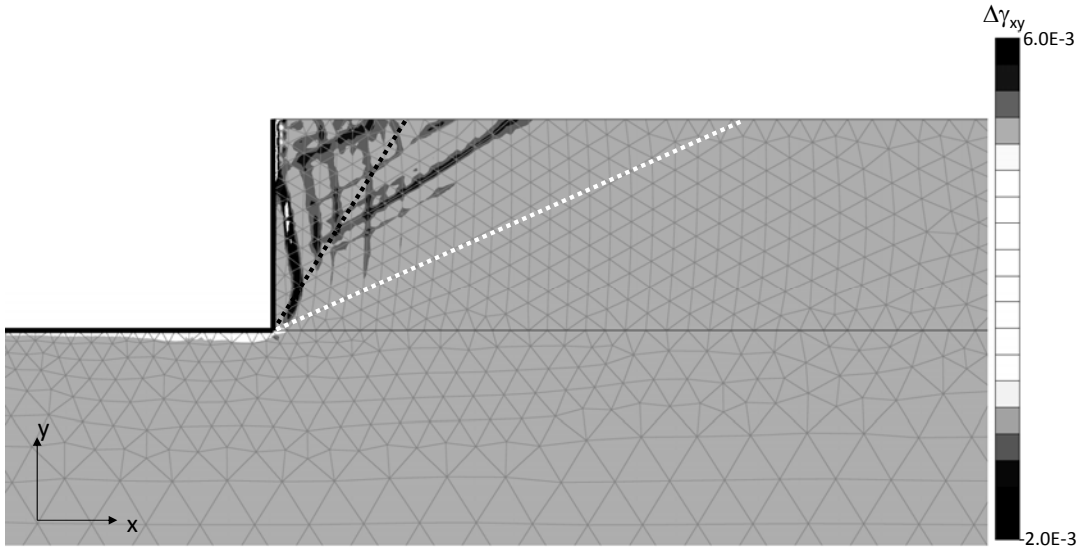

(c)

Fig. 4 Shear strain increments for (a) static condition, (b) $k_h = 0.3$ g, and (c) $k_h = 0.5$ g. Red and yellow dotted lines indicate the theoretical failure planes calculated by the Coulomb and M-O methods, respectively

Table 2 Summary of shaking table test and tilted test

No.	Source	Case	Wall type	Wall height	Load	Observed θ	k_{max} [1]	k_{eq} [2]	k_{eq} / k_{max}
1	Koseki *et al.* (1998a)	S-2	Cantilever	53 cm	Sinusoidal	55°	NA	NA	–
2	Koseki *et al.* (1998a)	S-3	Gravity	53 cm	Sinusoidal	59°	NA	NA	–
3	Koseki *et al.* (1998a)	S-4	Leaning	53 cm	Sinusoidal	51°	NA	NA	–
4	Koseki *et al.* (1998a)	S-5	Leaning	53 cm	Sinusoidal	50°	NA	NA	–
5	Koseki *et al.* (1998a)	S-6	Leaning	53 cm	Sinusoidal	49°	NA	NA	–
6	Koseki *et al.* (1998a)	T-8	Leaning	53 cm	Pseudo-static	51°	NA	NA	–
7	Watanabe *et al.* (2003)	Case 1	Cantilever	53 cm	Seismic	62°	0.78	NA	
8	Watanabe *et al.* (2003)	Case 2	Gravity	53 cm	Seismic	54°	0.94	NA	–
9	Watanabe *et al.* (2003)	Case 3	Leaning	53 cm	Seismic	47°	0.93	NA	–
10	Watanabe *et al.* (2011)	Case 1	Gravity	53 cm	Seismic	52°	0.98	0.75	0.76
11	Watanabe *et al.* (2011)	Case 2	Gravity	53 cm	Seismic	56°	0.95	0.75	0.79
12	Watanabe *et al.* (2011)	Case 3	Gravity	53 cm	Seismic	58°	1.00	0.83	0.82
13	Watanabe *et al.* (2011)	Case 4	Gravity	53 cm	Seismic	55°	0.92	0.82	0.89
14	Watanabe *et al.* (2011)	Case 5	Gravity	53 cm	Seismic	NA	0.97	0.79	0.81

[1] PGA of input motion normalized by gravity

[2] PGA of averaged motions within the failure wedge normalized by gravity

Toyoura sand is used as the backfill and subsoil layers in all tests. At a low confining pressure (9.8 kPa), the shear resistance angle φ of Toyoura sand is 51° and 44° according to the plane strain compression test and triaxial test (Tatsuoka *et al.* 1991). The observed failure angle at the center of the model is 3° to 7° less than that measured at the side wall because of the friction of the side wall. The curved failure planes indicate that the soil response is not under fully plane strain conditions. Therefore, the friction angle from the trixial test (44°) is used to calculate the theoretical failure angle at the static condition ($k_h = 0$). The interface friction angle (δ) between the subsoil and the wall is assumed equal to 0.75 φ (= 38°). Figure 5 shows the comparison between the calculated failure angle and observed failure angle. We also calculate the theoretical failure angle given the maximum input acceleration ($k_h = k_{max}$) by using the M-O method. The results are compared with the observed angle (Fig. 5). The observed failure angle is obviously closer to the angle calculated for the static condition than that calculated by the M-O method. However, the calculated failure angle for the static condition is still higher than the observed failure angle (*i.e.*, the wedge size is underestimated).

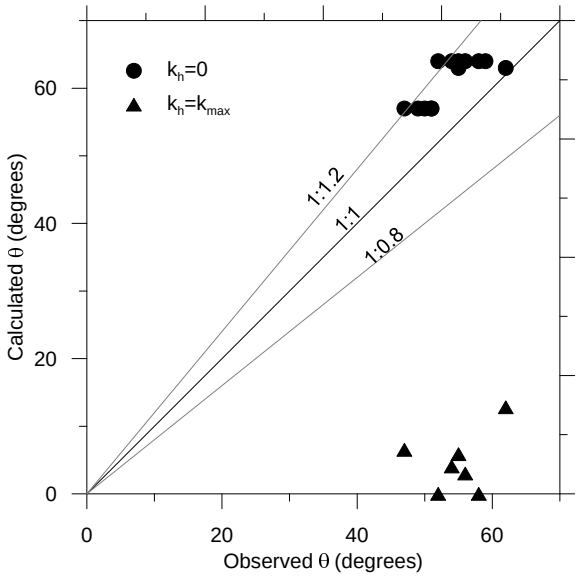

Fig. 5 Comparison of failure angle from experiments and theoretical M-O calculation

4. PROPOSED PROCEDURE

We propose a simple procedure to estimate seismically induced earth pressure on the basis of case histories, laboratory modeling, and FEM simulation. In the M-O method, the size of the critical wedge increases with increasing seismic coefficient. Thus, seismic earth pressure increments increase rapidly and are potentially overestimated. By contrast, case histories, FEM analysis, and experiments demonstrate that the size of the critical wedge has limited changes for different seismic loadings. Moreover, the observed failure plane is similar to the theoretical plane without considering any seismic load. Therefore, similar to the S-W method, this study proposes a fixed-wedge procedure to over-

come the current limitations of the M-O method. The fixed wedge behind the wall is determined under the static condition. This concept is comparable to the common practice where yield acceleration is obtained by using a fixed critical surface. The proposed procedure to calculate the total active thrust P_{AE} includes two steps:

1. A Coulomb analysis is performed to obtain the critical wedge under the static condition. The critical wedge can be determined by obtaining θ in the following equation:

$$\cot(\theta-\beta) = -\tan(\alpha-\beta+\delta+\varphi) + \frac{1}{\cos(\alpha-\beta+\delta+\varphi)}\sqrt{\frac{\sin(\varphi+\delta)\cos(\alpha+\delta)}{\cos(\alpha-\beta)\sin(\varphi-\beta)}} \quad (7)$$

The weight of the wedge (W) can be calculated as follows:

$$W = \frac{\gamma H^2}{2(\tan\theta-\tan\beta)}(1+\tan\alpha\tan\beta)(1+\tan\alpha\tan\theta) \quad (8)$$

2. Limit-equilibrium analysis is performed under a pseudo-static condition with the critical wedge determined from Step 1. The seismic earth force on the retaining wall can be calculated by the equilibrium of all forces acting on the wedge (shown in Fig. 1), which yields the equation below:

$$P_{AE} = \frac{\sin(\theta-\varphi)W + \cos(\theta-\varphi)Wk_h}{\cos(\delta+\alpha-\theta+\varphi)} \quad (9)$$

5. VERIFICATION AND DISCUSSION

5.1 Shaking Table Measurement

The proposed method is first used to calculate the seismic earth pressures to compare with the shaking table measurement by Watanabe *et al.* (2011) in Fig. 6. The seismic earth pressure at the point of the maximum measured resulting force on the wall is presented in terms of the seismic earth pressure increment coefficient ΔK_{AE} against free-field (input motion) PGA as the seismic coefficient. The curves obtained through the M-O and S-W solutions are also presented, and the free-field PGA is adopted as the seismic coefficient k_h to calculate ΔK_{AE}. Both the M-O and S-W methods overestimate the measured seismic earth pressures in varying degrees. By contrast, the estimated values of the proposed procedure agrees well with the measured values even though the fixed-wedge approach slightly underestimates the size of the failure wedge as mentioned in section 3.3. One confounding factor is that the equivalent acceleration in the soil wedge is lower than the acceleration of input motions. The maximum value of the measured equivalent acceleration (k_{eq}) within the soil wedge is around 80% of the PGA of the input motion (k_{max}) (Table 2). Thus, the use of higher seismic coefficients directly from the input motion compensates for the underestimation of the wedge size in the calculation of seismic earth pressures. The NCHRP report (Anderson *et al.* 2009) suggested a reduction of free-field acceleration to obtain equivalent acceleration within soil wedges for estimating seismic soil pressure. The scaling for the scattering factor is dependent on the wall height and characteristics of input motions. Considering a wall height of 6.5 m, the equivalent acceleration ranges between 70% to 95% of the PGA of the input motion, which is consistent with the observation by Watanabe *et al.* (2011). However, such a reduction requires a careful evaluation and is not widely adopted in design practice. By contrast, the proposed approach, which uses free-field motion in conjunction with the fixed wedge from the static condition, is simple and yields reasonable results.

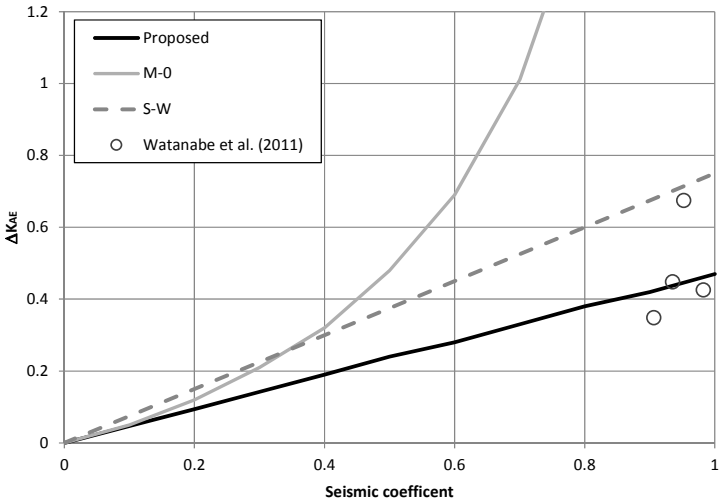

Fig. 6 Comparison of seismic earth pressure increments through different approaches and observations

5.2 Centrifuge Measurement

In this section, the proposed approach will be verified by centrifuge experiments (Al Atik and Sitar 2010; Sitar *et al.* 2012). The models measure acceleration, displacement, bending moments, and earth pressures. However, no failure plane orientations are reported. One set of experiments involve a 6.5 m-high (prototype) U-shaped cantilever wall (designed for the Bay Area Rapid Transit Systemand Valley Transportation Authority) with sand backfill. Another set of experiments involved a 6.5 m prototype of the California Department of Transportation cantilever wall (Caltrans 2010) with sand or clay backfill. The PGA of the input motions ranges from 0.1 g to 0.87 g, and the predominant period ranges from 0.2 s to 0.62 s, thus spanning a broad range of ground motion characteristics for verifying our approach.

Figures 7 and 8 reproduce their experimental results in the same way as the seismic earth pressure increment coefficient ΔK_{AE}, against the free-field (input motion) PGA as the seismic coefficient. The ΔK_{AE} presented by Al Atik and Sitar (2010) and Sitar *et al.* (2012) is the maximum earth pressure back-calculated from the maximum measured moment in the wall structures rather than the direct maximum measurement by flexible pressure sensors. Therefore, this reported value includes the contribution of the inertia force of the wall and seismic earth pressure; hence, this value is higher than the actual earth pressure. Although no failure planes are reported, seismic earth pressure increment still increases linearly with seismic coefficient, thus implying that the size of the critical wedge remains unchanged regardless of the magnitude of seismic coefficients.

The seismic earth pressure increments calculated by the proposed approach are compared against the measurements in Figs. 7 and 8. The curves obtained through the M-O and S-W

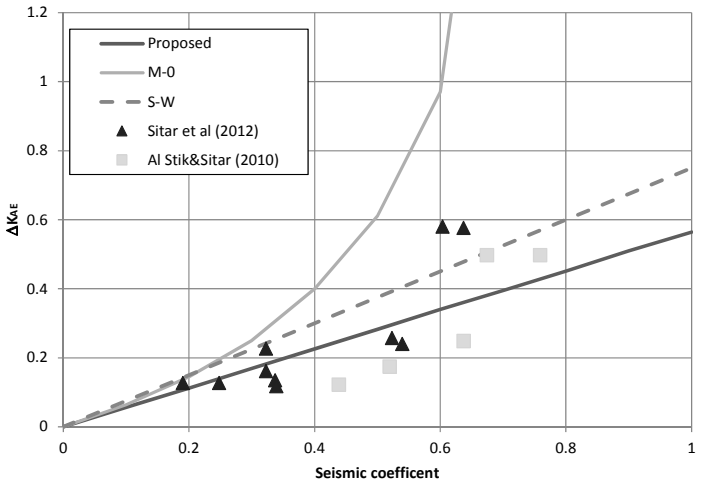

Fig. 7 Seismic earth pressure increments in the case of the U-shaped wall

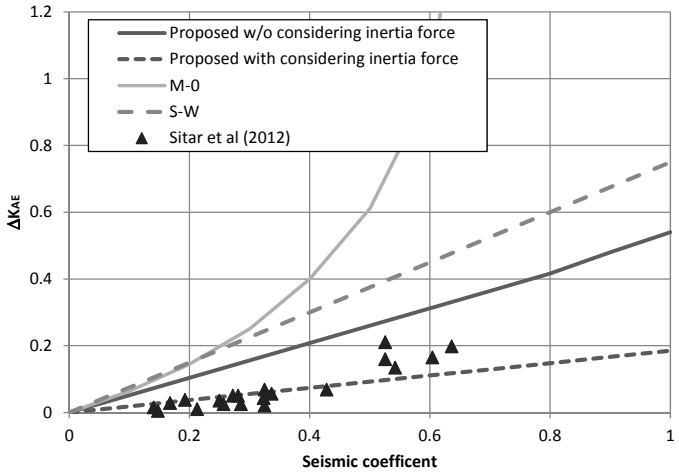

Fig. 8 Seismic earth pressure increments in the case of the cantilever wall

solutions are also presented, and PGA is adopted as seismic coefficient k_h to calculate ΔK_{AE}. For the case of the U-shaped wall (Fig. 7), the estimated value from the proposed approach agrees with those obtained in the centrifuge test, whereas the results from the M-O method deviate from the experiment results once k_h is greater than 0.3 g. However, both results of the proposed approach and the M-O solution are consistently higher than that of the centrifuge test in the case of the cantilever wall (Fig. 8), because the calculated force is acting on the wedge plane rather than on the wall, as measured in the centrifuge test (Fig. 9). The seismic force can be reduced further by the presence of soil between the wall and critical wedge. Al Atik and Sitar (2010) and Athanasopoulos-Zekkos *et al.* (2013) reported that the movements of the wall and soil are out of phase under seismic conditions. We can assume from the findings that soil wedge ABC in Fig. 9 has a phase movement close to that of the wall (*i.e.*, different from the phase movement of critical wedge ACD). Therefore, the force on the wall can be reduced further by the inertia force acting on the opposite direction of the P_A. By subtracting the inertia force of soil wedge ABC (estimated as the weight of

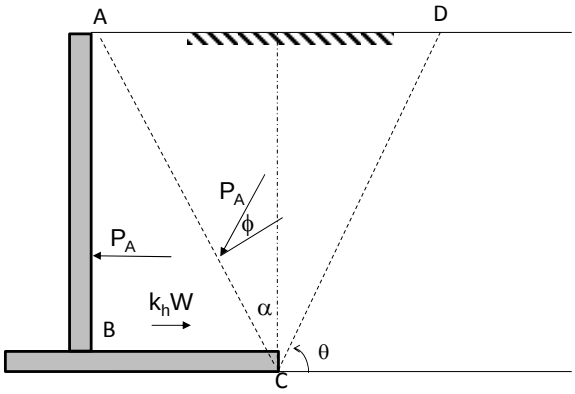

Fig. 9 Illustration of seismic force reduced by inertia force on the cantilever wall

the wedge multiplied by k_h) the calculated seismic force increment agrees well with the measurement obtained by the centrifuge test (Fig. 8). However, such force reduction is only applicable to a seismic case because of the inertia forces involved. The force on the wall and on the wedge is the same in the static condition because no inertia force is present.

In summary, the proposed approach can reasonably estimate seismic earth pressure for a wide range of conditions. The proposed approach is considered acceptable for the following reasons regardless if this approach underestimates a few measured points from the centrifuge tests: (1) the reported value of the centrifuge test is higher than the actual earth pressure because it includes both the soil pressure and inertia force of structures; (2) the maximum earth pressure compared herein occurs shortly and only once. The maximum earth pressure does not have sufficient duration to cause significant wall movements, and the effective earth pressure is low.

6. CONCLUSIONS

Case history data and recent experiment data indicate that current methods for evaluating seismically induced lateral earth pressure are conservative and can potentially lead to overdesign. This paper reviewed these commonly used methods and identified the limitations of the M-O method, wherein the critical wedge is dependent on the shaking intensity. Thus, the estimated earth pressure becomes irrationally high and the method becomes inoperative when the seismic load exceeds a certain limit.

On the basis of observed failure planes from recent case histories, experiments by other researchers, and numerical simulations in this study, we conclude that the potential failure wedge changes insignificantly in size under different shaking intensities because of strain localization. Therefore, this study proposed a fixed-wedge approach to rationally calculate seismic earth pressure for engineering practice. The fixed wedge is determined from the static condition and should be used with the seismic coefficient from free-field motion without considering the scattering factor. The earth pressures calculated by the proposed simple procedure agree well with recent experiments. Hence, the fixed-wedge approach is recommended in lieu of the M-O method.

ACKNOWLEDGEMENTS

This study was supported by the National Science Council under Award Number NSC102-2625-M-005-004. The authors gratefully acknowledge the support provided by the council.

REFERENCES

AASHTO, American Association of State Highway and Transportation Officials (2013). *AASHTO LRFD Bridge Design Specifications*.

Al Atik, L. and Sitar, N. (2010). "Seismic earth pressure on cantilever retaining structures." *Journal of Geotechnical and Geoenvironmental Engineering*, **136**, 1324–1333.

Anderson, D.G., Martin, G.R., Lam, I., and Wang, J.N. (2009). *Seismic Analysis and Design of Retaining Walls, Buried Structures, Slopes, and Embankments*. NCHRP Rep. 611.

Athanasopoulos-Zekkos, A., Vlachakis, V.S., and Athanasopoulos, G.A. (2013). "Phasing issues in the seismic response of yielding, gravity-type earth retaining walls – Overview and results from a FEM study." *Soil Dynamics and Earthquake Engineering*, **55**, 59–70. doi: 10.1016/j.soildyn.2013.08.004

Caltrans, California Department of Transportation. (2010). *Standard Plans: Retaining Wall Type 1 - H = 4' through 30'*, Plan No. B3-1.

Clough, G.W. and Fragaszy, R.F. (1977). "A study of earth loadings on floodway retaining structures in the 1971 San Fernando Valley earthquake." *6th World Conference on Earthquake Engineering*.

Fang, H.-Y. (1991). *Foundation Engineering Handbook*, 2nd Ed., New York, Chapman & Hall.

Fang, Y.S., Yang, Y.C., and Chen, T.J. (2003). "Retaining walls damaged in the Chi-Chi earthquake." *Canadian Geotechnical Journal*, **40**, 1142–1153.

Gazetas, G., Psarropoulos, P.N., Anastasopoulos, I., and Gerolymos, N. (2004). "Seismic behavior of flexible retaining systems subjected to short-duration moderately strong excitation." *Earthquake Engineering*, **24**, 537–550.

JRA, Japanes Road Association. (1987). *Earthworks Manual-Re-Taining Wall, Culverts, and Temporary Structure*.

Kontoe, S., Pelecanos, L., and Potts, D. (2013). "An important pitfall of pseudo-static finite element analysis." *Computers and Geotechnics*, **48**, 41–50.

Koseki, J., Munaf, Y., Tatsuoka, F., Tateyama, M., Kojima, K., and Sato, T. (1998a). "Shaking and tilt table tests of geosynthetic-reinforced soil and conventional-type retaining walls." *Geosynthetics International*, **5**, 73–98.

Koseki, J., Tatsuoka, F., Munaf, Y., Tateyama, M., and Kojima, K. (1998b). "A modified procedure to evaluate active earth pressure at high seismic loads." *Soils and Foundations*, **S2**, 209–216.

Lew, M., Simantob, E., and Hudson, M.E. (1995). "Performance of shored earth retaining systems during the January 17, 1994 Northridge earthquake." *Recent Advances in Geotechnical Earthquake Engineering and Soil Dynamics*, St. Louis.

Mononobe, N. and Matsuo, M. (1929). "On the determination of earth pressures during earthquakes." *Proc. World Engineering Congress*.

Nakamura, S. (2006). "Re-examination of Mononobe-Okabe theory of gravity retaining walls using centrifuge model tests." *Soils and Foundations*, **46**(2), 135–146.

Okabe, S. (1926). "General theory of earth pressures." *Journal of Japan Society of Civil Engineers*, **12**(1), 123–134.

Psarropoulos, P.N., Klonaris, G., and Gazetas, G. (2005). "Seismic earth pressures on rigid and flexible retaining walls." *International Journal of Soil Dynamics and Earthquake Engineering*, **25**, 795–809.

Seed, H.B. and Whitman, R.V. (1970). "Design of earth retaining structures for dynamic loads." *Specialty Conf. on Lateral Stresses in the Ground and Design of Earth Retaining Structures*, ASCE, Cornell Univ., Ithaca, N.Y.

Sitar, N., Mikola, R.G., and Candia, G. (2012). "Seismically induced lateral earth pressures on retaining structures and basement wall." *Geocongress*, Oakland, USA.

Tatsuoka, F., Okahara, M., Tanaka, T., Tani, K., Morimoto, T., and Siddiquee, M.S.A. (1991). "Progressive failure and particle size effect in bearing capacity of a footing on sand." *Geotechnical Engineering Congress*, Boulder, Colorado, USA.

Tatsuoka, F., Tateyama, M., and Koseki, J. (1996). "Performance of soil retaining walls for railway embankements." *Soils and Foundations*, Special Issue on Geotechnical Aspects of the January 17, 1995 Hyogoken-Nanbu Earthquake, 311–324.

Tatsuoka, F., Koseki, J., Tateyama, M., Munaf, Y., and Horii, K. (1998). "Seismic stability against high seismic loads of geosynthetic-reinforced soil retaining structures." *6th International Conference on Geosynthetics*, Atlanta, **1**, 103–142.

Terzaghi, K. (1920). "Old earth-pressure theory and new test results." *Egineering News Record*, **85**(14), 632–637.

Watanabe, K., Koseki, J., and Tateyama, M. (2011). "Seismic earth pressure exerted on retaining walls under a large seismic load." *Soils and Foundations*, **51**(3), 379-394.

Watanabe, K., Munaf, Y., Koseki, J., Tateyama, M., and Kojima, K. (2003). "Behaviors of several types of model retaining walls subjected to irregular excitation." *Soils and Foundations*, **43**(5), 13–27.